

Life and extinction of megafauna in the ice-age Arctic

Daniel H. Mann^{a,1}, Pamela Groves^b, Richard E. Reanier^c, Benjamin V. Gaglioti^d, Michael L. Kunz^e, and Beth Shapiro^{f,1}

^aGeosciences Department, University of Alaska, Fairbanks, AK 99775; ^bInstitute of Arctic Biology, University of Alaska, Fairbanks, AK 99775; ^cReanier & Associates, Inc., Seattle, WA 98166; ^dWater and Environmental Research Center, University of Alaska, Fairbanks, AK 99775; ^eCooperative Extension and Resources, University of Alaska, Fairbanks, AK 99775; and ^fDepartment of Ecology and Evolutionary Biology and University of California, Santa Cruz Genomics Institute, University of California, Santa Cruz, CA 95064

Edited by Richard G. Klein, Stanford University, Stanford, CA, and approved September 23, 2015 (received for review June 29, 2015)

Understanding the population dynamics of megafauna that inhabited the mammoth steppe provides insights into the causes of extinctions during both the terminal Pleistocene and today. Our study area is Alaska's North Slope, a place where humans were rare when these extinctions occurred. After developing a statistical approach to remove the age artifacts caused by radiocarbon calibration from a large series of dated megafaunal bones, we compare the temporal patterns of bone abundance with climate records. Megafaunal abundance tracked ice age climate, peaking during transitions from cold to warm periods. These results suggest that a defining characteristic of the mammoth steppe was its temporal instability and imply that regional extinctions followed by population reestablishment from distant refugia were characteristic features of ice-age biogeography at high latitudes. It follows that long-distance dispersal was crucial for the long-term persistence of megafaunal species living in the Arctic. Such dispersal was only possible when their rapidly shifting range lands were geographically interconnected. The end of the last ice age was fatally unique because the geographic ranges of arctic megafauna became permanently fragmented after stable, interglacial climate engendered the spread of peatlands at the same time that rising sea level severed former dispersal routes.

ice age | megafauna | extinction | paleoecology | mammoth steppe

One of the most intriguing examples of mass extinction and the most accessible in terms of its geological record occurred around the end of the Wisconsin ice age ca. 10–45 calendar ka B.P. (10,000–45,000 calendar y ago) when some 65% of terrestrial megafauna genera (animals weighing >45 kg) became globally extinct (1). Based on what we know about recent species extinctions, the causes of extinction are usually synergistic, often species-specific, and therefore, complex, which implies that there is no universal explanation for end-Pleistocene extinctions (2, 3). Globally and specifically in the Arctic (3–10), megafaunal extinctions have been variously blamed on overhunting, rapid climate change, habitat loss, and introduced diseases (3–10). Further complicating a clear understanding of the causes of ice-age extinctions is that the magnitude and tempo of environmental change during the last 100,000 y of the Pleistocene were fundamentally different than during the Holocene (11), and these differences had far-reaching implications for community structure, evolution, and extinction causes (12).

A recent survey comparing the extinction dates of circum-boreal megafauna with ice-age climate suggests that extinctions and genetic turnover were most frequent during warm, interstadial events (13). However, the mechanisms for these extinctions remain unclear, partly because this previous study considered multiple taxa living in many different ecosystems. Here, we focus on five megafaunal species that cohabited a region of the Arctic with an ecological setting that is relatively well-understood. To avoid the methodological problems involved in pinpointing extinction dates (13), we infer population dynamics from changes in the relative abundance of megafauna over time. Using a uniquely large dataset of dated megafaunal bones from one particular area, we test a specific paleoecological hypothesis relating rapid climate change to population dynamics—namely, that transitions from cold to warm intervals were briefly optimal for grazing megafauna.

The study area is Alaska's North Slope, the tundra region bordered to the south by the Brooks Range and to the north by the Arctic Ocean (Fig. 1). The North Slope is a particularly interesting place to study end-Pleistocene extinctions for several reasons. First, its ice-age megafauna included iconic species like woolly mammoth (*Mammuthus primigenius*), steppe bison (*Bison priscus*), and cave lion (*Panthera spelaea*) (14). Second, the local extinctions of megafauna on Alaska's North Slope occurred at a time when archaeological remains are rare, suggesting that people seldom ventured there (15, 16). Third, bone preservation in arctic environments tends to be excellent because of the presence of permafrost (perennially frozen ground), which makes it possible to ¹⁴C date large numbers of bones from many different species (SI Appendix, Table S1). Our record of dated bones provides key insights into the temporal dynamics and biogeographical characteristics of the mammoth steppe, a biome that was unique to the ice ages and the exact nature of which has been long debated (17).

Background

Mammoth Steppe. Episodically during the late Pleistocene, the mammoth steppe extended from Europe to northwestern Canada (18). Its soils were relatively dry, warm, and fertile compared with those of the present day (19, 20) (SI Appendix, SI Text), and its vegetation supported large herds of grazing mammals in species-rich communities (14, 17, 18). The biomasses and diversities of these ice-age communities contrast starkly with the impoverished megafaunal communities living in the same regions today (10, 21). The climate supporting the mammoth steppe was more continental than today (18) and, as detailed below, it was much more changeable at millennial and centennial timescales.

The nature and, for some authors, even the veracity of the mammoth steppe remain controversial (14, 17). Some paleobotanists

Significance

Understanding species extinction is a major concern today, and past extinctions provide valuable lessons. Numerous mammal species became extinct in the Arctic at the end of the ice age, but it is unclear why. By comparing numbers of dated bones with climate records, we find that megafaunal species, like mammoth, horse, and bison, experienced boom and bust cycles during the ice age as they tracked rapid climate changes. For these species to persist, long-distance dispersal was necessary. Their extinction on the North Slope occurred as the ice age ended, because rising sea level severed dispersal routes and spreading peat simultaneously degraded range quality. This finding suggests that arctic mammals can be resilient to environmental changes but only if their habitats remain widely interconnected.

Author contributions: D.H.M., M.L.K., and B.S. designed research; D.H.M., P.G., B.V.G., M.L.K., and B.S. performed research; D.H.M., P.G., and R.E.R. contributed new analytic tools; P.G. and R.E.R. analyzed data; and D.H.M., P.G., R.E.R., B.V.G., and B.S. wrote the paper.

The authors declare no conflict of interest.

This article is a PNAS Direct Submission.

Freely available online through the PNAS open access option.

¹To whom correspondence may be addressed. Email: bashapir@ucsc.edu or dhmann@alaska.edu.

This article contains supporting information online at www.pnas.org/lookup/suppl/doi:10.1073/pnas.1516573112/-DCSupplemental.

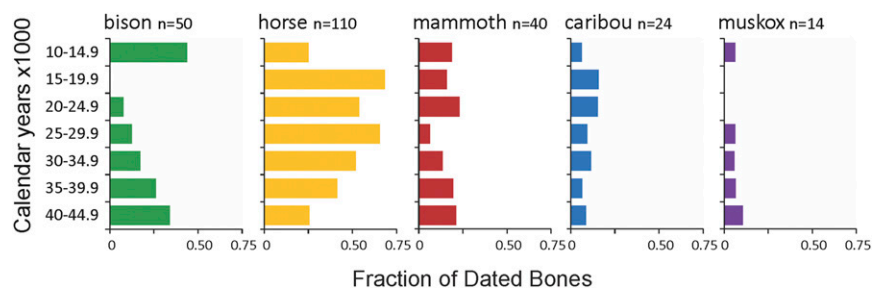


Fig. 3. Changes in the relative abundances of megafaunal herbivore taxa on the North Slope of Alaska between 10,000 and 45,000 calendar y B.P. Details of these ^{14}C dates are given in *SI Appendix, Table S1*.

- iii) Widespread paludification took place during lengthy interstadials.
- iv) Megafaunal diets shifted in response to widespread paludification during these long-lasting interstadials.
- v) Population declines caused by the spread of organic soils during lengthy interstadials caused population bottlenecks among arctic megafauna that are recorded by changes in gene frequencies.

Distinguishing Calibration Noise in Cumulative Probability Distributions of ^{14}C Dates. To test the warm transitions were briefly optimal hypothesis, we need to compare temporal trends in megafaunal abundance with climate records. Cumulative probability distributions (CPDs) of ^{14}C dates can be informative proxies for changes in abundance through time, and they have been widely used in paleontology, archaeology, and geomorphology (6, 40–42). Unfortunately, the interpretation of CPDs is complicated by artifacts introduced during the calibration of ^{14}C dates to calendar ages by variations in slope of the curve relating ^{14}C age to calendar age (42–44) (*SI Appendix, SI Text*). Here, we use a Monte Carlo-based approach to separate data-derived peaks in CPDs from calibration-induced noise. This method compares the CPD of a set of real calibrated dates with the CPDs of multiple simulated sets of calibrated dates to identify peaks in bone abundance that are unlikely to result from calibration artifacts. If the warm transitions were briefly optimal hypothesis is correct, peaks in megafaunal abundance should coincide with the warm interstadials, specifically the initial stages of interstadial warming.

Results

The relative abundances of herbivorous megafaunal species living on the North Slope of Alaska shifted markedly through time (Fig. 3). Horses increased in relative abundance after 40 calendar ka B.P., whereas muskoxen were apparently absent between 15 and 25 calendar ka B.P. along with steppe bison between 15 and 20 calendar ka B.P. The combined CPD of 263 megafaunal bones

dating to between 10 and 45 calendar ka B.P. has numerous peaks (Fig. 4). The curve loses some of this spiky character before 30 calendar ka B.P., because the range of possible calibrated ages increases as error terms of individual dates increase.

The Monte Carlo procedure allows us to identify peaks in the bone-abundance curve that are not caused by calibration effects. Eight of the peaks in the CPD rise above the calibration noise at the $P \leq 0.05$ level, suggesting that these eight peaks were times of unusually abundant megafauna (Fig. 4). In general, peaks in megafaunal abundance coincide with warm, mid-Wisconsin interstadials between 30 and 50 calendar ka B.P. The most recent peak in abundance occurred during GI-1e, which in northwest Europe, was manifested as the Bølling–Allerød warm period.

The $\delta^{15}\text{N}$ values of horse bone collagen reflect dietary changes over time (45). On the North Slope, starting ca. 47 calendar ka B.P. and ending at 10 calendar ka B.P., *Equus* bone collagen $\delta^{15}\text{N}$ values became increasingly less positive, with values changing from +8‰ to +10‰ between 30 and 47 calendar ka B.P. to from +1‰ to +2‰ at the time of extirpation ca. 12.6 calendar ka B.P. (Fig. 5).

Discussion

Comparing Bone Abundance to Climate. Although peaks in bone abundance generally coincide with warm interstadials, correlations differ slightly according to which proxy record is compared (Fig. 6). Some of these differences are caused by the dating uncertainties present in all of the records, and others probably reflect real differences in how global climate trends were expressed in different regions. Of the three proxy records, methane (CH_4) is the most globally applicable because of its rapid mixing in the atmosphere. Compared with the CH_4 record, megafauna populations peaked on the North Slope during GI-12, -11, -8, -6–7, -5, -4, and -1. Another bone peak occurred at the outset of GI-2 at ca. 24 calendar ka B.P. (Fig. 6).

Comparison of bone abundances with $\delta^{18}\text{O}$ records from speleothems in southeast China suggests similar correlations (Fig. 6, *Middle*), with peaks in megafaunal abundance early in GI-1 and -2.

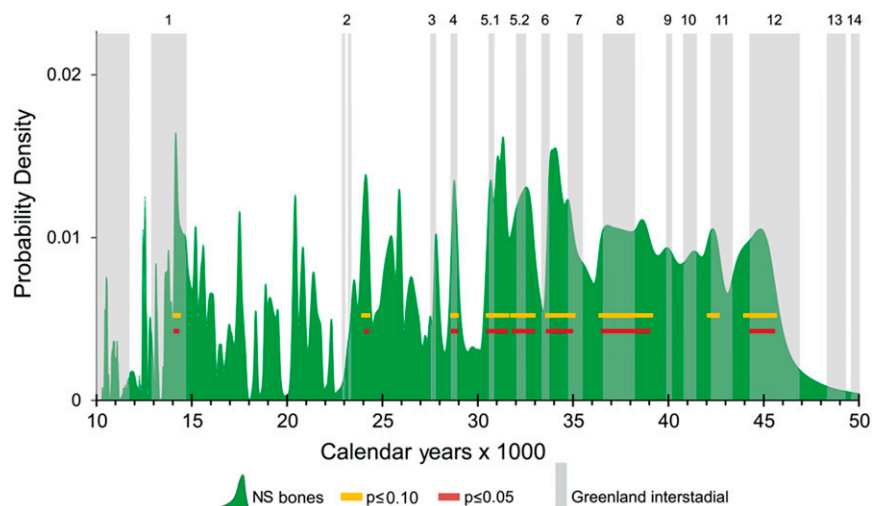


Fig. 4. The CPD of 263 calibrated ages of North Slope (NS) megafaunal bones (solid green). Yellow bars mark times when there is a $P \leq 0.10$ of the peaks in bone abundance being explicable as artifacts of the ^{14}C calibration process. Red bars mark peaks where $P \leq 0.05$. Vertical gray bars depict the Greenland Interstadials (GIs) after Rasmussen et al. (47).

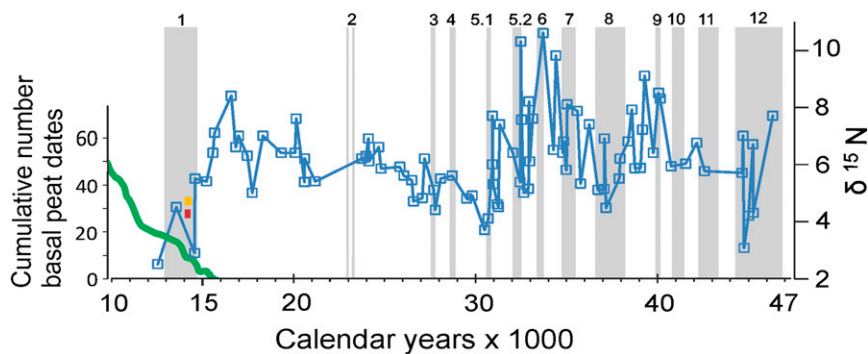


Fig. 5. The $\delta^{15}\text{N}$ of 90 bones of caballine horses of differing ages from Alaska's North Slope. The numbered columns show the GIs. The green line shows the cumulative number of basal peat dates from Alaska (72). Red and yellow bars show the timing of the bone abundance peak in the early stages of GI-1. Horse diet changed radically as peat spread during GI-1. Similar shifts in diet occurred during some of the earlier interstadials. Bone ages are plotted by their median calibrated ages.

A bone peak ca. 28.5–29 calendar ka B.P. may correlate to the beginning of GI-3, although this particular interstadial is not recorded clearly in the Chinese record. There are suggestions that bone peaks also occurred during the initial stages of GI-11, -8, and -6. Comparisons to the Greenland Ice Core Project (GRIP) $\delta^{18}\text{O}$ record suggest that bone peaks occurred during GI-1, -4, -5.1, -5.2, -8, and -12 (Fig. 6, *Bottom*). A bone peak occurred at the onset of GI-2.2, and a similar timing is suggested for GI-5.1 and possibly, GI-10.

Testing the Warm Transitions Were Briefly Optimal Hypothesis.

Prediction 1: Megafaunal abundance peaked during warm interstadial periods, particularly during their initial stages. The youngest interstadials, GI-2.2 and -1, are of particular interest because the precision of age control in both the ice-core records and the ^{14}C dating technique decline with age (46, 47) (*SI Appendix, SI Text*). The warming trend culminating in GI-2.2 began ca. 24 calendar ka B.P. (Fig. 6). The peak in bone abundance at 23.9–24.3 calendar ka B.P. occurred, therefore, during its earliest stages. In the CH_4 and Chinese $\delta^{18}\text{O}$ records, peak megafaunal abundance occurred in the initial stages of GI-1. In the GRIP $\delta^{18}\text{O}$ record, this same bone peak falls during the warmest part of GI-1 but is still within the first millennium of this lengthy interstadial. These correlations tend to confirm predictions made by the hypothesis by Guthrie (37).

Prediction 2: In the course of the most recent interstadial, the Bolling-Allerød (GI-1), megafaunal abundance declined as paludification progressed. Consistent with this prediction, the bone peak occurring ca. 14 calendar ka B.P. ended ~1,100 y before GI-1 terminated (Fig. 6). Furthermore, it coincided with the initial rapid spread of peat across the North Slope and preceded the widespread paludification occurring later (Fig. 5) (31).

Prediction 3: Widespread paludification took place during lengthy interstadials. Peat layers dating to mid-Wisconsin interstadials are widespread in both Siberia and Alaska (48). In northwest Alaska, peat layers and elevated percentages of spruce pollen suggest that paludification accompanied the intermittent presence of forests there between 40 and 60 calendar ka B.P. (49). On Siberia's Lena River Delta, buried peat layers date to 32–52 calendar ka B.P. (45). Along the Kolyma River, peat-rich buried soils date to 44–46, 40–43, 36, and 32 calendar ka B.P. (50), and on the New Siberian Islands, buried soils suggest that paludification occurred at 73° N during some mid-Wisconsin interstadials (51). These reports confirm that paludification was widespread in the Arctic during at least some interstadials, suggesting that a short-lived grazing bonanza followed by the spread of peat may have occurred during lengthy (>1,000 y) interstadials.

Prediction 4: Megafaunal diets shifted in response to widespread paludification during lengthy interstadials. At the outset of GI-1, the shift from mammoth steppe to the moist tundra vegetation accompanying widespread paludification coincided with a striking change in the diet of horses (Fig. 5). Similar shifts in $\delta^{15}\text{N}$ occurred earlier during several of the longest interstadials, including GI-8, which lasted 1,640 y, and GI-12, which lasted 2,580 y (47). Declining $\delta^{15}\text{N}$ during interstadials is consistent with paludification's impact on vegetation composition, soil temperature, soil moisture, and rooting depths of plants (10, 52).

Prediction 5: Population declines caused by the spread of organic soils during lengthy interstadials caused population bottlenecks among arctic megafauna that are recorded by changes in gene frequencies. Consistent with this prediction, paleontological records and aDNA indicate that population bottlenecks affected a number of megafaunal species at high latitudes between 36 and 48 calendar ka B.P., the interval that saw some of the longest interstadials. Noncaballine

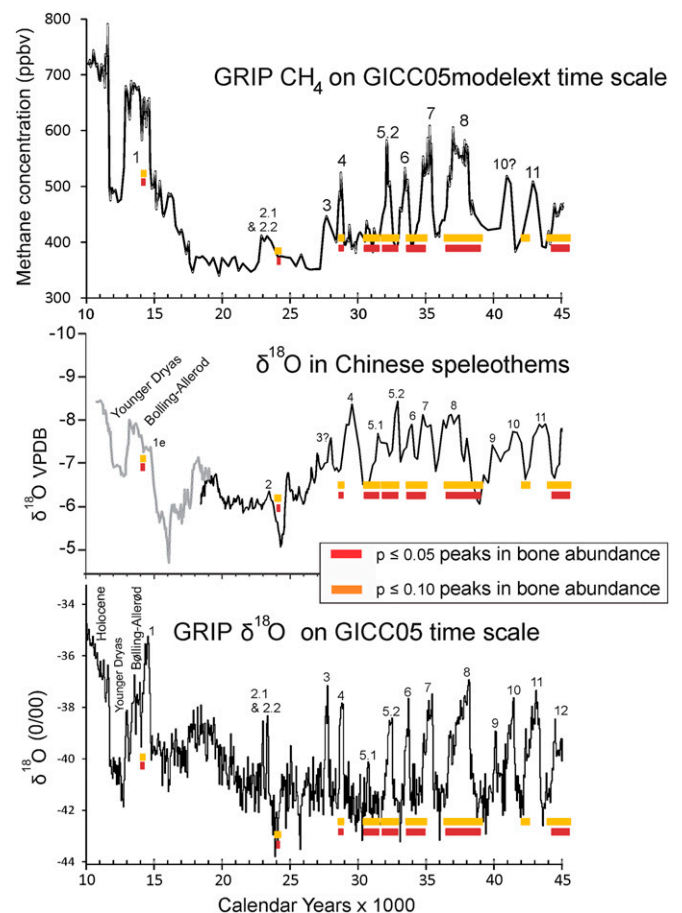


Fig. 6. Comparisons between peaks in megafaunal bone abundance and climate proxy records. The terminology and timing of the GIs are from Rasmussen et al. (47). (*Top*) Methane concentrations in the GRIP core (47). (*Middle*) The $\delta^{18}\text{O}$ record from Chinese speleothems (73). The dynamics of $\delta^{18}\text{O}$ in southeast China are dominated by changing evaporative source areas and transport distances of precipitation. (*Bottom*) $\delta^{18}\text{O}$ in the GRIP core (47). The close correlation between the CH_4 record and the $\delta^{18}\text{O}$ record attests to the global extent of the climatic events recorded in Greenland. ppbv, Parts per billion by volume; VPDB, Vienna Pee Dee Belemnite.

horses became extinct in Alaska ca. 36 calendar ka B.P. (53). Based on aDNA, Alaskan brown bears experienced a significant population decline around that same time (54). Ancient DNA further suggests the numbers of steppe bison, horses, and mammoths living at high latitudes decreased markedly 35–45 calendar ka B.P. (3, 55, 56). Also based on aDNA, population bottlenecks affected cave lions sometime after 50 calendar ka B.P. (57) and muskoxen after 48 calendar ka B.P. (3, 58). Although the precise timing of these population bottlenecks remain obscure (13), their occurrence during the mid-Wisconsin interstadials is consistent with the hypothesis by Guthrie (37). We interpret these bottlenecks as side effects of widespread paludification during lengthy interstadials, such as GI-14, -12, and -8.

Synthesis

Accepting the warm transitions were briefly optimal hypothesis (Fig. 2) leads to new inferences concerning the nature of the mammoth steppe, the biogeography of its megafaunal inhabitants, and the probable causes of their end-Pleistocene extinctions.

Mammoth Steppe: A Biome Defined by Its Instability. Concurrence between peaks in numbers of bones and periods of climatic transitions implies the occurrence of boom and bust cycles in ice-age megafaunal populations in arctic Alaska (Fig. 6). Changes in the abundance of taxa through time—for instance, the absence of bison between 15 and 20 calendar ka B.P. (Fig. 3)—suggest the occurrence of regional-scale extinctions followed by recolonization. Megafaunal populations were fluctuating because the ecosystems supporting them were changing. Together with the global climate records (Fig. 6), our data suggest that short-term (10^1 – 10^3 y) ecological instability was a characteristic feature of the mammoth steppe in arctic Alaska during the last ice age.

Like an azonal soil that never equilibrates with regional climate and has properties that are, instead, determined by the nature and timing of the last geomorphic or ecological disturbance, the mammoth steppe may have been an azonal biome that never fully equilibrated to any single climate state. If true, this implies that, in addition to being a spatial mosaic of ecosystems (26), the mammoth steppe was also a temporal mosaic with soils, vegetation, and fauna that were chronically engaged in ecological successions triggered by repeated, short-lived, and radical shifts in climate. One reason that no clear analogs of the mammoth steppe exist today may be simply that the degree of climatic instability experienced at high latitudes during the late Pleistocene is absent today.

Ice-Age Dispersability Imperative. Survival in an azonal biome requires coping with incessant environmental change, and arctic megafauna may have been forced to play a game of musical chairs across continental distances. Survival would have been especially challenging for populations dependent on either long-distance migration, like some caribou herds are today in northern Alaska, or episodic long-distance dispersal between shifting locations of suitable habitat. In Africa today, the regional persistence of elephant populations depends on episodic dispersals of subpopulations between patches of favorable habitat, often across hundreds of kilometers (59). During some Pleistocene stadials (14), mammoth steppe covered a region three times that of sub-Saharan Africa, and the very un-Holocene tempo of ice-age climate change meant that patches of suitable forage were flickering in and out of existence every few centuries. The imperative may have been to disperse or be extirpated.

Fatal Intersection of Events. With this dispersability imperative in mind, the intersection of two events made GI-1 (the Bølling-Allerød) uniquely fatal for megafauna in arctic Alaska. First, paludification had ample time to transform soils and vegetation over this interstadial's 1,800-y span (Fig. 5). Second, relative sea level was rising rapidly, reducing the land area of northern Alaska, weakening the continentality of the climate, and blocking dispersal routes to Siberia.

The degree of isolation between Alaska and Siberia established after 14 calendar ka B.P. was extreme compared with most of the late Pleistocene. The Bering Land Bridge was finally

submerged between 12 and 13 calendar ka B.P. (60, 61) when sea level surpassed the –50-m level, a height not reached for the previous 40,000 y. By the early Holocene, relative sea level stood higher along the coast of northern Alaska than it had at any time in the previous 100,000 y (62, 63).

As the Bering Land Bridge was closing, the ice-free corridor between the Cordilleran and Laurentide Ice Sheets was slowly opening. The corridor may have first appeared 13.5–14 calendar ka B.P. (64), but it probably remained ecologically impassable to megafauna until after GI-1 ended ca. 12.9 calendar ka B.P. (55, 65, 66). The end of the last ice age was probably uniquely fatal for arctic megafauna because of the unusual intersection of two events: widespread paludification that drastically reduced range quality for megafaunal grazers and simultaneously hindered their ability to disperse across the resulting soggy landscape and flooding of dispersal routes to Asia before the ice-free corridor leading to lower-latitude North America fully opened.

Materials and Methods

^{14}C Dating of Bones and Analysis of Bone $\delta^{15}\text{N}$. We dated 496 bones from disarticulated skeletons on Alaska's North Slope (10) (*SI Appendix, SI Text and Table S1*). These bones were in good condition and were identified by their definitive morphological characteristics. In certain instances, temporal and ecological assumptions were used in our identifications (*SI Appendix, Table S1*). Bone collagen was dated by accelerator MS techniques without ultrafiltration (*SI Appendix, SI Text*). We excluded bones with nonfinite ages, bones of extant taxa that were <10 calendar ka B.P. in age, and bones with finite ages >43,500 ^{14}C y B.P., and included 41 previously published bone dates from the North Slope that met these criteria (10). We therefore use 263 megafaunal bones to make CPDs for comparison with proxy records of climate change. The species composition of these 263 bones is 113 caballine horses, 52 steppe bison, 40 woolly mammoths, 26 caribou, 16 tundra muskoxen, 7 cave lions, 3 moose, 2 wolves (*Canis lupus*), 2 saiga antelope (*Saiga tatarica*), 1 short-faced bear (*Arctodus simus*), and 1 brown bear. We described the changing species composition of the megafauna through time by calculating the percentage of the total number of bones of each taxon where median-calibrated ages fall within 5,000-y age bins between 10 and 45 calendar ka B.P. Smaller bin sizes tended to distort abundance trends because of the spiky nature of the dated bone record. We measured $\delta^{15}\text{N}$ in bone collagen of ^{14}C -dated horse bones using an Elemental Analyzer Isotope Mass Spectrometer.

Distinguishing Calibration Noise in CPDs of ^{14}C Dates. Some peaks and valleys in the CPDs of calibrated ^{14}C dates are artifacts resulting from the calibration process (*SI Appendix, SI Text*). We use a Monte Carlo approach to distinguish which peaks in a CPD of ^{14}C dates are not caused by calibration noise. We calibrated the ^{14}C dates using the OxCal program [version 4.2.4 (67)] and the IntCal13 calibration curve (68) to produce a summed CPD. For the simulated datasets, we cannot simply produce sets of randomly chosen ^{14}C dates; unlike randomly chosen calendar ages, every ^{14}C age is not equally likely, because randomly chosen ^{14}C ages are not uniformly distributed in calendar time (*SI Appendix, SI Text*). Instead, we generate 999 sets of 263 random calendar ages using OxCal from the time interval corresponding to 9,310–43,100 ^{14}C y B.P. Error estimates for each of these simulated dates come from a regression equation relating SD to calendar age in the real bone dataset. We next use the R_Simulate procedure in OxCal to assign a ^{14}C date and an error term to each of the randomly chosen calendar ages. These simulated ^{14}C dates are calibrated using R_Simulate to create 999 CPDs containing 263 calibrated dates each in 5-y bins, which then become the Monte Carlo trials against which the CPD of the real $n = 263$ calendar ages is compared. Finally, we estimate how extreme the upper-tail probability of the actual bone CPD is with respect to the CPDs of the randomly generated dates. We calculate empirical P values by tallying the number of times 999 simulated probability values in each bin equaled or exceeded the bone data values using the relation $P = (r + 1)/(n + 1)$, where r is the number of random values greater than or equal to the observed bone value, and n is the number of randomly generated datasets (69, 70). The timespans where $P \leq 0.05$, for example, define time periods when the bone CPD peaks are different from what would be expected by chance at the $\alpha = 0.05$ level. This procedure allows us to identify peaks in the CPD that warrant comparison with climate proxy data.

ACKNOWLEDGMENTS. We thank D. Meltzer and D. Guthrie for useful discussion. Comments by two anonymous reviewers improved an earlier version of this manuscript. This research was supported by grants from the Bureau of Land Management and the National Science Foundation Grants PLR-1417036 and PLR-1417611.

1. Barnosky AD, Koch PL, Feranec RS, Wing SL, Shabel AB (2004) Assessing the causes of late Pleistocene extinctions on the continents. *Science* 306(5693):70–75.
2. Meltzer DJ (2015) Pleistocene overkill and North American mammalian extinctions. *Annu Rev Anthropol* 44:33–53.
3. Lorenzen ED, et al. (2011) Species-specific responses of Late Quaternary megafauna to climate and humans. *Nature* 479(7373):359–364.
4. MacPhee RD, Marx PA (1997) The 40,000-year plague. Humans, hyperdisease, and first-contact extinctions. *Natural Change and Human Impact in Madagascar*, eds Goodman S, Patterson B (Smithsonian Institution, Washington, DC), pp 169–217.
5. Nogués-Bravo D, Rodríguez J, Hortal J, Batra P, Araújo MB (2008) Climate change, humans, and the extinction of the woolly mammoth. *PLoS Biol* 6(4):e79.
6. Nikolskiy PA, Sulerzhitsky LD, Pitulko VV (2011) Last straw versus Blitzkrieg overkill: Climate-driven changes in the Arctic Siberian mammoth population and the Late Pleistocene extinction problem. *Quat Sci Rev* 30(17–18):2309–2328.
7. Stuart AJ, Lister AM (2011) Extinction chronology of the cave lion *Panthera spelaea*. *Quat Sci Rev* 30(17–18):2329–2340.
8. Stuart AJ, Lister AM (2012) Extinction chronology of the woolly rhinoceros *Coelodonta antiquitatis* in the context of late Quaternary megafaunal extinctions in northern Eurasia. *Quat Sci Rev* 51:1–17.
9. MacDonald GM, et al. (2012) Pattern of extinction of the woolly mammoth in Beringia. *Nat Commun* 3:893.
10. Mann DH, Groves P, Kunz ML, Reanier RE, Gaglioti BV (2013) Ice-age megafauna in Arctic Alaska: Extinction, invasion, survival. *Quat Sci Rev* 70:91–108.
11. Roy K, Valentine JW, Jablonski D, Kidwell SM (1996) Scales of climatic variability and time averaging in Pleistocene biotas: Implications for ecology and evolution. *Trends Ecol Evol* 11(11):458–463.
12. Hewitt GM (2004) Genetic consequences of climatic oscillations in the Quaternary. *Philos Trans R Soc Lond B Biol Sci* 359(1442):183–195.
13. Cooper A, et al. (2015) Paleoeecology. Abrupt warming events drove Late Pleistocene Holarctic megafaunal turnover. *Science* 349(6248):602–606.
14. Guthrie RD (1990) *Frozen Fauna of the Mammoth Steppe: The Story of Blue Babe* (University of Chicago Press, Chicago).
15. Kunz ML, Reanier RE (1994) Paleoindians in Beringia Evidence from arctic Alaska. *Science* 263(5147):660–662.
16. Goebel T, Waters MR, O'Rourke DH (2008) The late Pleistocene dispersal of modern humans in the Americas. *Science* 319(5869):1497–1502.
17. Hopkins DM, Matthews JV, Schweger CE (1982) *Paleoecology of Beringia* (Academic, New York).
18. Guthrie RD (2001) Origin and causes of the mammoth steppe: A story of cloud cover, woolly mammal tooth pits, buckles, and inside-out Beringia. *Quat Sci Rev* 20(1–3):549–574.
19. Young SB (1982) The vegetation of land-bridge Beringia. *Paleoecology of Beringia*, eds Hopkins DM, Matthews JV, Schweger CE, Young SB (Academic, New York), pp 179–194.
20. Walker DA, et al. (2001) Calcium-rich tundra, wildlife, and the “Mammoth Steppe.” *Quat Sci Rev* 20(1–3):149–163.
21. Zimov SA, Zimov NS, Chapin FS, III (2012) The past and future of the mammoth steppe ecosystem. *Paleontology in Ecology and Conservation*, ed Louys J (Springer, Berlin), pp 193–225.
22. Ritchie JC, Cwynar LC (1982) The late Quaternary vegetation of the north Yukon. *Paleoecology of Beringia*, eds Hopkins DM, Matthews JV, Schweger CE, Young SB (Academic, New York), pp 113–126.
23. Elias SA, Short SK, Birks HH (1997) Late Wisconsin environments of the Bering Land Bridge. *Palaeogeogr Palaeoclimatol Palaeoecol* 136(1–4):293–308.
24. Elais SA, Berman D, Alfimov A (2000) Late Pleistocene beetle faunas of Beringia: Where east meets west. *J Biogeogr* 27(6):1349–1363.
25. Zazula GD, et al. (2006) Vegetation buried under Dawson tephra (25,300 14C years BP) and locally diverse late Pleistocene paleoenvironments of Goldbottom Creek, Yukon, Canada. *Palaeogeogr Palaeoclimatol Palaeoecol* 242(3–4):253–286.
26. Zazula GD, Froese DG, Elias SA, Kuzmina S, Mathewes RW (2007) Arctic ground squirrels of the mammoth-steppe: Paleoeecology of late Pleistocene middens (~24000–29450 14 C yr BP), Yukon Territory, Canada. *Quat Sci Rev* 26(7–8):979–1003.
27. Blinnikov MS, Gaglioti BV, Walker DA, Wooller MJ, Zazula GD (2011) Pleistocene graminoid-dominated ecosystems in the Arctic. *Quat Sci Rev* 30(21–22):2906–2929.
28. Haile J, et al. (2009) Ancient DNA reveals late survival of mammoth and horse in interior Alaska. *Proc Natl Acad Sci USA* 106(52):22352–22357.
29. Mann DH, Reanier RE, Peteet DM, Kunz ML (2001) Environmental change and arctic paleoindians. *Arctic Anthropol* 38(2):119–138.
30. Bartlein PJ, et al. (2015) Early-Holocene warming in Beringia and its mediation by sea-level and vegetation changes. *Clim Past Discuss* 11(2):873–932.
31. Mann DH, Peteet DM, Reanier RE, Kunz ML (2002) Responses of an arctic landscape to late glacial and early Holocene climatic changes: The importance of moisture. *Quat Sci Rev* 21(8–9):997–1021.
32. Chapin FS, III, Matson PA, Vitousek P (2011) *Principles of Terrestrial Ecosystem Ecology* (Springer, Berlin).
33. Mack MC, Schuur EA, Bret-Harte MS, Shaver GR, Chapin FS (2004) Ecosystem carbon storage in arctic tundra reduced by long-term nutrient fertilization. *Nature* 431(7007):440–443.
34. Kade A, Walker DA (2008) Experimental alteration of vegetation on nonsorted circles: Effects on cryogenic activity and implications for climate change in the Arctic. *Arct Antarct Alp Res* 40(1):96–103.
35. Baughman CA, Mann DH, Verbyla D, Kunz ML (2015) Soil-surface organic layers in the Arctic Foothills: Distribution, development, and microclimatic feedbacks. *J Geophys Res: Biogeosci* 120(6):1150–1164.
36. Yu Z, Beilman DW, Jones MC (2009) *Sensitivity of Northern Peatland Carbon Dynamics to Holocene Climate Change. Carbon Cycling in Northern Peatlands*, Geophysical Monographs Series (AGU, Washington, DC), Vol 184, pp 55–69.
37. Guthrie RD (2006) New carbon dates link climatic change with human colonization and Pleistocene extinctions. *Nature* 441(7090):207–209.
38. Sumina OI (1994) Plant communities on anthropogenically disturbed sites on the Chukotka Peninsula, Russia. *J Veg Sci* 5(6):885–896.
39. Kade AN, Walker DA, Reynolds MK (2005) Plant communities and soils in cryoturbated tundra along a bioclimate gradient in the Low Arctic, Alaska. *Phytocoenologia* 35(4):761–820.
40. MacPhee RDE, et al. (2002) Radiocarbon chronologies and extinction dynamics of the late Quaternary mammalian megafauna of the Taimyr Peninsula, Russian Federation. *J Archaeol Sci* 29(9):1017–1042.
41. Mann DH, Meltzer DJ (2007) Millennial-scale dynamics of valley fills over the past 12,000 ¹⁴C yr in northeastern New Mexico, USA. *Geol Soc Am Bull* 119:1433–1448.
42. Williams AN (2012) The use of summed radiocarbon probability distributions in archaeology: A review of methods. *J Archaeol Sci* 39(3):578–589.
43. Guilderson TP, Reimer PJ, Brown TA (2005) Geoscience. The boon and bane of radiocarbon dating. *Science* 307(5708):362–364.
44. Contreras DA, Meadows J (2014) Summed radiocarbon calibrations as a population proxy: A critical evaluation using a realistic simulation approach. *J Archaeol Sci* 52:591–608.
45. Schirmer L, et al. (2002) Paleoenvironmental and paleoclimatic records from permafrost deposits in the Arctic region of Northern Siberia. *Quat Int* 89(1):97–118.
46. Svensson A, et al. (2008) A 60,000 year Greenland stratigraphic ice core chronology. *Clim Past Discuss* 4(1):47–57.
47. Rasmussen SO, et al. (2014) A stratigraphic framework for abrupt climatic changes during the Last Glacial period based on three synchronized Greenland ice-core records: Refining and extending the INTIMATE event stratigraphy. *Quat Sci Rev* 106:14–28.
48. Lozhkin AV, Anderson PM (2011) Forest or no forest: Implications of the vegetation record for climatic stability in Western Beringia during Oxygen Isotope Stage 3. *Quat Sci Rev* 30(17–18):2160–2181.
49. Wetterich S, et al. (2012) Late quaternary environmental and landscape dynamics revealed by a pingo sequence on the northern Seward Peninsula, Alaska. *Quat Sci Rev* 39:26–44.
50. Zanina OG, Gubin SV, Kuzmina SA, Maximovich SV, Lopatina DA (2011) Late-Pleistocene (MIS 3–2) palaeoenvironments as recorded by sediments, palaeosols, and ground-squirrel nests at Duvanny Yar, Kolyma lowland, northeast Siberia. *Quat Sci Rev* 30(17–18):2107–2123.
51. Andreev AA, et al. (2009) Weichselian and Holocene palaeoenvironmental history of the Bol'shoy Lyakhovsky Island, New Siberian Archipelago, Arctic Siberia. *Boreas* 38(1):72–110.
52. Stevens RE, Hedges REM (2004) Carbon and nitrogen stable isotope analysis of northwest European horse bone and tooth collagen, 40,000 BP-present: Palaeoclimatic interpretations. *Quat Sci Rev* 23(7–8):977–991.
53. Guthrie RD (2003) Rapid body size decline in Alaskan Pleistocene horses before extinction. *Nature* 426(6963):169–171.
54. Barnes I, Mathews P, Shapiro B, Jensen D, Cooper A (2002) Dynamics of Pleistocene population extinctions in Beringian brown bears. *Science* 295(5563):2267–2270.
55. Shapiro B, et al. (2004) Rise and fall of the Beringian steppe bison. *Science* 306(5701):1561–1565.
56. Debruyne R, et al. (2008) Out of America: Ancient DNA evidence for a new world origin of late quaternary woolly mammoths. *Curr Biol* 18(17):1320–1326.
57. Barnett R, et al. (2009) Phylogeography of lions (*Panthera leo* spp.) reveals three distinct taxa and a late Pleistocene reduction in genetic diversity. *Mol Ecol* 18(8):1668–1677.
58. Campos PF, et al. (2010) Ancient DNA analyses exclude humans as the driving force behind late Pleistocene musk ox (*Ovibos moschatus*) population dynamics. *Proc Natl Acad Sci USA* 107(12):5675–5680.
59. van Aarde RJ, Jackson TP (2007) Megaparks for metapopulations: Addressing the causes of locally high elephant numbers in southern Africa. *Biol Conserv* 134(3):289–297.
60. Brigham-Grette J, Gualtieri L (2004) Response to Grosswald and Hughes (2004), Brigham-Grette et al. (2003), “Chlorine-36 and 14C chronology support a limited last glacial maximum across central Chukotka, northeastern Siberia, and no Beringian ice sheet,” and Gualtieri et al. (2003), “Pleistocene raised marine deposits on Wrangel Island, northeastern Siberia: Implications for Arctic ice sheet history.” *Quat Sci Res* 62(2):227–232.
61. Keigwin LD, Donnelly JP, Cook MS, Driscoll NW, Brigham-Grette J (2006) Rapid sea-level rise and Holocene climate in the Chukchi Sea. *Geology* 34(10):861–864.
62. Waelbroeck C, et al. (2002) Sea-level and deep water temperature changes derived from benthic foraminifera isotopic records. *Quat Sci Rev* 21(1–3):295–305.
63. Hu A, et al. (2010) Influence of Bering Strait flow and North Atlantic circulation on glacial sea-level changes. *Nat Geosci* 3:118–121.
64. Dyke AS (2004) An outline of North American deglaciation with emphasis on central and northern Canada. *Quaternary Glaciations—Extent and Chronology, Part II: North America*, eds Ehlers J, Gibbard PL (Elsevier, Amsterdam), pp 373–424.
65. Burns JA (1996) Vertebrate paleontology and the alleged ice-free corridor: The meat of the matter. *Quat Int* 32:107–112.
66. Burns JA (2010) Mammalian faunal dynamics in late Pleistocene Alberta, Canada. *Quat Int* 217(1–2):37–42.
67. Bronk Ramsey C (2009) Bayesian analysis of radiocarbon dates. *Radiocarbon* 51(1):337–360.
68. Reimer PJ, et al. (2013) IntCal13 and Marine13 radiocarbon age calibration curves 0–50,000 years cal BP. *Radiocarbon* 55(4):1869–1887.
69. Davison AG, Hinkley DV (1997) *Bootstrap Methods and Their Applications* (Cambridge Univ Press, Cambridge, United Kingdom).
70. North BV, Curtis D, Sham PC (2002) A note on the calculation of empirical P values from Monte Carlo procedures. *Am J Hum Genet* 71(2):439–441.
71. Brigham-Grette J, Lozhkin AV, Anderson PM, Glushkova O (2004) Paleoenvironmental conditions in Western Beringia before and during the Last Glacial Maximum. *Entering America: Northeast Asia and Beringia Before the Last Glacial Maximum*, ed Madsen DB (University of Utah Press, Salt Lake City), pp 29–61.
72. Jones MC, Yu Z (2010) Rapid deglacial and early Holocene expansion of peatlands in Alaska. *Proc Natl Acad Sci USA* 107(16):7347–7352.
73. Wang YJ, et al. (2001) A high-resolution absolute-dated late Pleistocene monsoon record from Hulu Cave, China. *Science* 294(5550):2345–2348.